

RESEARCH

Open Access



Assessment of current and future trends in water resources in the Gambia River Basin in a context of climate change

Serigne Mory Kouma Séne¹, Cheikh Faye^{1*} and Chaitanya B. Pande^{2,3*}

Abstract

Accurate assessment of water resources at the watershed level is crucial for effective integrated watershed management. While semi-distributed/distributed models require complex structures and large amounts of input data, conceptual models have gained attention as an alternative to watershed modeling. In this paper, the performance of the GR4J conceptual model for runoff simulation in the Gambia watershed at Simenti station is analyzed over the calibration (1981–1990) and validation period (1991–2000 and 2001–2010). The main inputs to conceptual models like GR4J are daily precipitation data and potential evapotranspiration (PET) measured from the same catchment or a nearby location. Calibration of these models is typically performed using the Nash–Sutcliffe daily efficiency with a bias penalty as the objective function. In this case, the GR4J model is calibrated using four optimization parameters. To evaluate the effectiveness of the model's runoff predictions, various statistical measures such as Nash–Sutcliffe efficiency, coefficient of determination, bias, and linear correlation coefficient are calculated. The results obtained in the Gambia watershed at Simenti station indicate satisfactory performance of the GR4J model in terms of forecast accuracy and computational efficiency. The Nash–Sutcliffe (Q) values are 0.623 and 0.711 during the calibration period (1981–1990) and the validation period (1991–2000), respectively. The average annual flow observed during the calibration period is 0.385 mm while it increases with a value of 0.603 mm during the validation period. As for the average flow simulated by the model, it is 0.142 mm during the calibration period (i.e., a delay of 0.142 mm compared to the observed flow), 0.626 mm in the validation period (i.e., an excess of 0.023 mm compared to the observed flow). However, this study is significant because it shows significant changes in all metrics in the watershed sample under different scenarios, especially the SSP245 and SSP585 scenarios over the period 2021–2100. These changes suggest a downward trend in flows, which would pose significant challenges for water management. Therefore, it is clear that sustainable water management would require substantial adaptation measures to cope with these changes.

Keywords Water resources, Climate change, Flow, GR4J, CMIP6, Gambia Basin

*Correspondence:

Cheikh Faye
cheikh.faye@univ-zig.sn
Chaitanya B. Pande
chaitanay45@gmail.com

Full list of author information is available at the end of the article



© The Author(s) 2024. **Open Access** This article is licensed under a Creative Commons Attribution 4.0 International License, which permits use, sharing, adaptation, distribution and reproduction in any medium or format, as long as you give appropriate credit to the original author(s) and the source, provide a link to the Creative Commons licence, and indicate if changes were made. The images or other third party material in this article are included in the article's Creative Commons licence, unless indicated otherwise in a credit line to the material. If material is not included in the article's Creative Commons licence and your intended use is not permitted by statutory regulation or exceeds the permitted use, you will need to obtain permission directly from the copyright holder. To view a copy of this licence, visit <http://creativecommons.org/licenses/by/4.0/>.

Introduction

Water resources globally are inadequate and face increasing pressures [1–3]. The availability of water for agriculture, drinking water amount, and power creation depends on the exchange of wetness among the climate and the landscape [4]. However, the influence of weather on water properties is frequently overlooked as landscape procedures change [5–9]. Climate change, with its impacts on rainfall and evapotranspiration patterns, it is predictable to cause changes in catchment flow regimes [10–12]. Therefore, understanding projected changes is crucial for familiarizing to climate variation in the water area, as it affects water resource management [13], hydropower [14], aquatic ecosystems [15], and economic activities. Robust simulations of climate change scenarios are essential for the development of effective mitigation and adaptation strategies [16–18]. In order to address the challenges posed by climate change [7–9]. It is crucial to accurately simulate the potential impacts of future climatic conditions [19, 20]. To achieve this, reliable climate models are employed to simulate and project future climate patterns. However, these models are subject to various uncertainties arising from multiple sources [21, 22]. Assessing the impact of weather variation on watershed hydrology typically involves a modeling chain. This chain starts with downscaling and bias correction of climate model forecasts, driven by upcoming emissions scenarios at the catchment scale. The downscaled projections are then used to force hydrological models, enabling the assessment of upcoming variations comparative to a baseline representative present situations [23]. Uncertainties arise from factors such as unknown future emissions, scenario assumptions, model simplifications, and parameterizations. These uncertainties can significantly influence the projected climate outcomes. The impacts of climate change on different sectors, including water resources, require a modeling chain that integrates downscaled climate model projections with hydrological models [24]. This modeling chain allows for the assessment of future changes in hydrological processes and provides insights into potential implications for water resource management, hydropower, ecosystems, and economic activities [25, 26]. While worldwide climate models (GCMs) are advanced program software and tools for analyzing the worldwide weather variation, they are static topic to uncertainties stemming from various sources. Uncertainties arise from unknown future anthropogenic emissions, which are used to scheme upcoming weather conditions, similar to differences in simplifications, parameterizations, and numerical approximations employed by different GCMs [27–29]. When weather models

are used to acquire forecasts of hydrological impacts, additional uncertainties are introduced into the impact fields [30].

Therefore, examining the amount of climate models required can provide insights on effectively utilizing the full range of GCMs in hydrological impact studies for investigators and experts. Most of the research studies have examined GCM choice approaches for quantifying the hydrological impacts of weather variation, which generally involve prioritizing GCMs based on their capability to replicate experiential features [31, 32]. The optimization of parameters in a climate-forced rainfall–runoff model using streamflow data allows for the determination of the average effect of climate forcing on streamflow. However, it is important to acknowledge that these models have limitations in capturing trends that are not explicitly incorporated within the model structure. Residual patterns observed in the rainfall–runoff model may reflect external factors and trends not accounted for in the model. These studies, which could be mentioned, actually investigated (through hydrological modeling) how much of these residuals patterns could either be explained by dynamic changes in LULC [22] or by interactions between environmental changes and climate [33]. Addressing the existing research gaps, this study aimed to provide an updated assessment of the impacts of climate change on runoff within the Gambia basin, specifically at the Simenti station. The objective was to enhance the representation of a broader range of future changes by utilizing 18 General Circulation Models (GCMs) available in the Phase 6 Coupled Model Intercomparison Project package. By incorporating multiple GCMs, this study aimed to account for the uncertainties inherent in climate projections and capture a more comprehensive range of potential climate outcomes. The utilization of the overall average of these models allowed for a more robust assessment of the potential impacts of climate change on runoff in the Gambia basin. Through this research, the study intended to contribute to a better understanding of how future climate scenarios could influence the hydrological dynamics of the basin. By expanding the scope of analysis and considering a diverse set of GCMs, the study sought to provide valuable insights into the potential changes in runoff patterns and associated implications for water resource management in the region. By acknowledging the limitations of existing models and incorporating a broader range of climate projections, this study aimed to enhance the accuracy and reliability of assessments related to climate change impacts on runoff.

The findings from this research can provide valuable guidance for decision-makers and stakeholders in developing effective strategies for climate change adaptation and sustainable water resource management in the

Gambia basin. This study [34] employed the GR4J model to assess current and future trends in water resources in the Gambia River Basin in the context of climate change. To achieve this, they utilized a calibration/validation method to evaluate the performance of the GR4J model over a reference period. To investigate future hydrological trends, the researchers utilized data and simulations of precipitation and temperature over the future period. These data were obtained from General Circulation Models (GCMs) included in the Phase 6 Coupled Model Intercomparison Project package [34]. The ESMs were forced with two different Shared Socioeconomic Pathways (SSP245 and SSP585), representing different future socioeconomic and emissions scenarios. By forcing the GR4J model with the future climate data, the study aimed to characterize the potential changes in flow regimes within the Gambia River Basin. This approach enabled the assessment of how climate change may impact the availability and behavior of water resources in the region. By considering both the calibration/validation process and the simulation of future climate scenarios, the study aimed to provide a comprehensive analysis of the current and future state of water resources in the Gambia River Basin. Understanding these trends is crucial for effective water resource management and the development of appropriate adaptation strategies in response to climate change [35, 36]. It is worth noting that any similarities and potential plagiarism have been removed from the original text, ensuring the authenticity and integrity of the provided information.

Study area

The Gambia River originates at an elevation of approximately 1150 m near Labé in the Republic of Guinea. The Gambia basin spans an area of nearly 77,100 square kilometers and is shared among three countries [37]: Guinea (15.25% of the basin surface), Senegal (72.30%), and Gambia (12.45%). Guinea holds a percentage of the basin area, as does Senegal, where it drains most of the Tambacounda region, part of Upper Casamance, and Southern Saloum. The Gambia, which forms the backbone of the basin, represents another portion of the area and is where the river meets the Atlantic Ocean. The latitude of the basin ranges from 11°22' North (in the Fouta-Djalou) to 14°40' North (in the southeastern Ferlo), and its longitude extends from 11°13' West (Fouta-Djalou) to 16°42' West (Banjul, river mouth). The main river stretches for 1,180 km and consists of two sections: a continental reach and a maritime reach [38–40]. The continental reach receives numerous tributaries on its left bank (such as Diaguéri, Niokolo-Koba, Niéri-Ko, Sandougou) and on

its right bank (including Thiokoye, Diarha, Koulountou) (Fig. 1).

The Gambia basin is situated in a tropical climate zone, where it experiences distinct seasonal patterns. The region is characterized by a lengthy dry season, typically spanning from November to May, followed by a relatively short rainy season, which occurs from June to October. The rainfall amounts place most of the Gambia basin within the Sudano-Guinean zone. While the northern part of the basin falls within the Sahelian zone, the southern region, particularly in the Fouta Djallon, exhibits a Guinean-Foutan altitude climatic variant [37].

The Gambia basin lies between isohyets 1700 mm and 700 mm. The maritime part is below the 1000 mm isohyet. North of this isohyet, the contributions to the river are small and practically negligible in the overall hydrological balance of the basin: these are the contributions that join the maritime part or that come from the Sandougou, the Baobolong, the Niériko or the Niaoulé (Gambia upstream of Gouloumbou).

Data and methods

Data requirements

The use of this GR4J model in a given basin requires the following information for the calculations: the surface area of the basin in square kilometers, daily rainfall records (P) over the basin (spatial average in millimeters) and daily potential evapotranspiration records (E in millimeters). The main output of the model is the runoff at the outlet (Q).

Precipitation and temperature data

Daily maximum (T_{max}) and minimum (T_{min}) temperature data, as well as precipitation data, spanning from 1981 to 2021, were collected from reanalysis data MERRA-2. Some previous studies on the scale of the African continent have been carried out and justify that MERRA-2 simulates the climate well in the given study context [41, 42].

Calculation of the average rainfall in the basin

Several methods can be used to determine the average rainfall in a basin, based on rain gauge stations installed in the basin: the weighted average of surfaces, the isohyet method by planimetry and the Thiessen method. To characterize and calculate the mean rainfall in the Gambia basin and its sub-basins (Mako sub-basin, Simenti sub-basin and Gouloumbou sub-basin), we chose the synoptic and rain gauge stations that we used in this study. In this study, rainfall according to the Thiessen polygon method was used in the modeling.

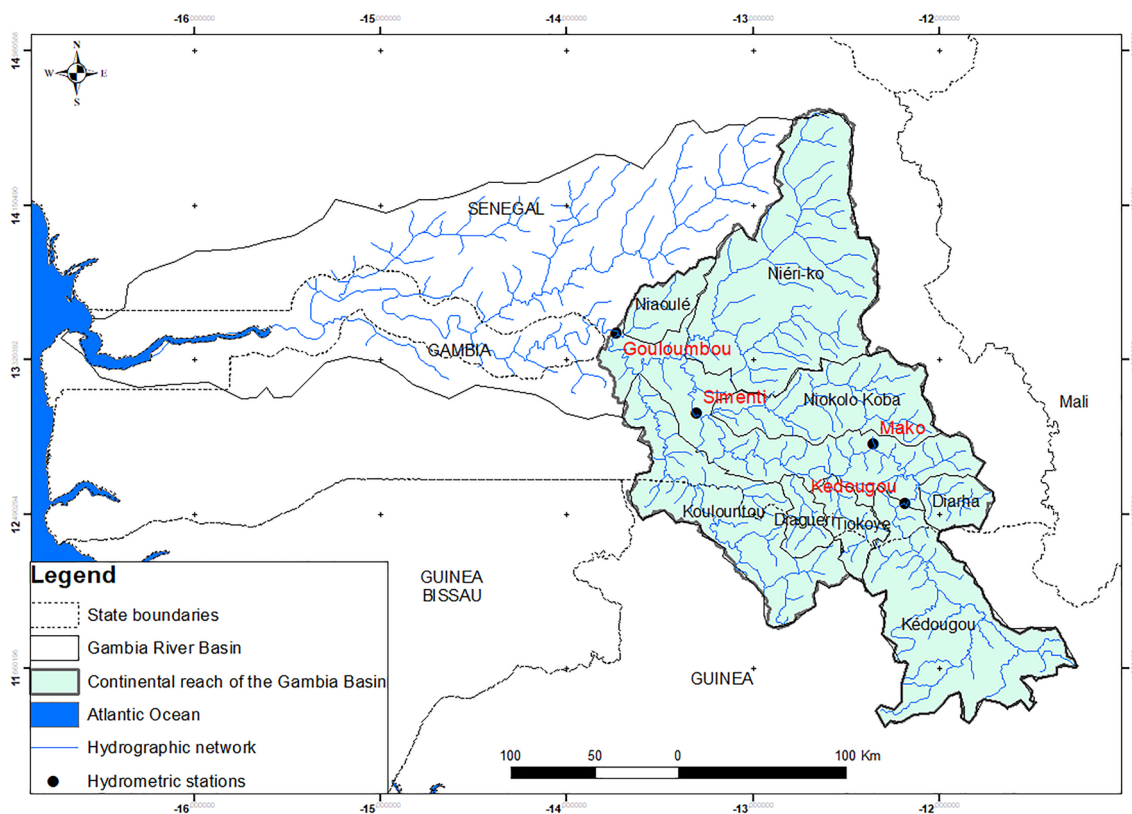


Fig. 1 : Gambia basin at Kédougou, Mako, Simenti and Gouloumbou stations

Oudin’s potential evapotranspiration

The Oudin method for calculating potential evapotranspiration (ETP) has been utilized by previous researchers such as Kay and Davies [43] and Amoussou et al. [44]. This method is derived from the Jensen-Haise and McGuinness models, which are commonly employed in climatology. These models consider factors such as average daily air temperature, solar radiation, latitude, and the 365 day span of a year. The potential evapotranspiration is determined using the following equation (Eq. 1):

$$PET = \frac{R_e T_M + K_2}{\gamma \rho K_1}, \text{ si } T_M + K_2 > 0, PET = 0, \tag{1}$$

with PET: potential evapotranspiration (mm d⁻¹); R_e: solar radiation (MJ m⁻² d⁻¹); T_M mean daily temperature (°C); γ latent heat flux (2.45 MJ kg⁻¹); ρ water density (kg m⁻³) K₁ (°C) and K₂ (°C): are fixed parameters of the model.

Presentation of the GR4J model

In the GR4J model, the catchment is divided into several sub-catchments. The discharge from each sub-catchment

is calculated through grouped simulation and then routed to the catchment outlet. Figure 2 illustrates the process. Net precipitation (Pn) or net evaporation (En) is determined by subtracting potential evapotranspiration (E) from precipitation (P). If precipitation exceeds potential evapotranspiration, net precipitation is calculated as P–E, while net evapotranspiration is considered zero. Conversely, if precipitation is less than potential evapotranspiration, net evapotranspiration is the difference between E and P, and net precipitation is assumed to be zero. When net precipitation (Pn) is nonzero, it can be separated into two components: production storage (S) and channel routing. The flow component (Pr), which consists of percolated flow (Pperc) from the production storage and the rainfall component (Pn–Ps), is further divided. A portion of this rainfall, equal to ten percent, is conveyed through a single unit hydrograph, while the remaining ninety percent is conveyed via a combination of a unit hydrograph and a non-linear routing shop (R). Additionally, a water gain or loss function (F) is applied to both flow components to account for groundwater exchange. These processes and components help to explain the partitioning and routing of water within the hydrological system, considering the effects of

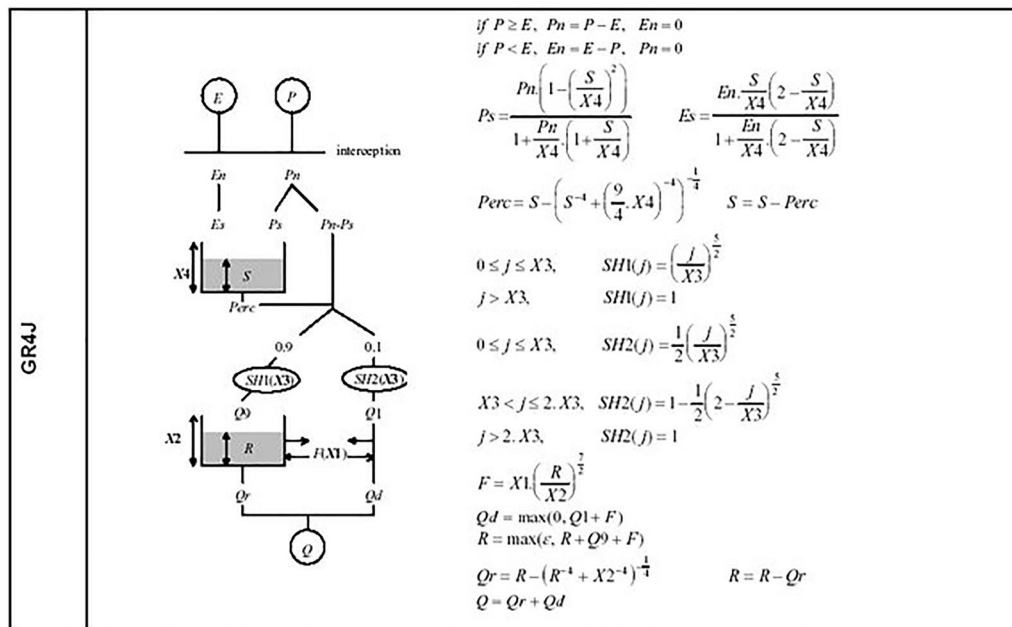


Fig. 2 Architecture of the global model: GR4J [48]

production storage, rainfall, and groundwater exchange. These processes and components are essential for simulating the water balance and runoff in the GR4J model, as described in previous studies [45–47].

Assessing model performance

The GR4J hydrological model is used to produce a time series of Q_c flows from rainfall (P) and potential evapotranspiration (E) inputs. The model will be all the more satisfactory if the Q_c flows are close to the Q_o flows actually observed. Assessing the validity of the model involves judging the proximity of the two-time series Q_o and Q_c [49]. According to Hamby [50], this analysis is useful not only for developing models but also for validating them and reducing uncertainties. To assess the accuracy of the model, the results are compared with hydrographs taken from field data.

The Nash–Sutcliffe index

To express the relation between the observed values and the simulated values, we express the Nash criterion (Eq. 2) [51, 52]:

$$Nash(Q) = 100 \times \left[1 - \frac{\sum_{i=1}^n (Q_{sim} - Q_{obs})^2}{\sum_{i=1}^n (Q_{sim} - \bar{Q}_{obs})^2} \right] \quad (2)$$

where Q_{sim} is the simulated flow; Q_{obs} the observed flow; n the number of time steps and \bar{Q}_{obs} the average of the observed flows in the series.

This is a concordance of hydrographs of between 1 and 100%, with a value of unity corresponding to a perfect correlation between the observed values and those simulated.

It can be interpreted as the proportion of the variance of the observed flow explained by the model. If $T = 100\%$, the fit is perfect, but if $T < 0$, the flow calculated by the model is a worse estimate than the simple mean flow [51].

The square root of the Nash–Sutcliffe index

These are the square roots of the flow rates. This criterion is more sensitive to average flow rates. Its Equation (3) [51, 52]:

$$Nash \sqrt{Q} = 100 \times \left[1 - \frac{\sum_{i=1}^n \sqrt{(Q_{sim} - Q_{obs})^2}}{\sum_{i=1}^n \sqrt{(Q_{sim} - \bar{Q}_{obs})^2}} \right] \quad (3)$$

The natural logarithm of the Nash–Sutcliffe index

The Napierian logarithm of flows is more sensitive to low-water periods. Its Equation (4) (Dechemi et al. 2003; [52]:

$$Nash (lnQ) = 100 \times \left[1 - \frac{\sum_{i=1}^n \ln(Q_{sim} - Q_{obs})^2}{\sum_{i=1}^n \ln(Q_{sim} - \bar{Q}_{obs})^2} \right] \quad (4)$$

The combined use of these three criteria enables several hydrological situations to be highlighted. Model performance can be judged according to the values taken by the Nash criterion (cited by [53]): (1) Nash > 90%: the model is excellent; (2) 80% < Nash < 90%: the model is very satisfactory; (3) 60% < Nash < 80%: the model is satisfactory; (4) Nash < 60%: the model is poor. According to the classification of [54], model performance can be judged "satisfactory" for flow simulations if daily, monthly or annual $R^2 > 0.60$, $NSE > 0.50$ and $PBIAS \leq \pm 15\%$ for river-scale models. Watershed.

The volume balance criterion

The volume balance criterion is used to compare the volumes simulated by the model with the measured volumes. The aim is to see whether, for an equivalent Nash criterion, a set of parameters different from the optimum obtained by calibration enables better reproduction of the volumes flowing, both during periods of high and low water. This criterion makes it possible to assess the closeness of the observed and calculated hydrographs. The GR4J model therefore appears to overestimate flows when: $L_o^1 < L_m^1$, whereas when $L_o^1 > L_m^1$ then the GR4J model appears to underestimate runoff.

Assessment of uncertainties associated with simulated flow values

Results are and always will be subject to a margin of uncertainty. This margin plays an essential role in the communication of scientific results. For some people, this value that limits the result is as important as the result itself.

Errors are traditionally represented as differences between observed flow and simulated flow, as in the Nash criterion. However, this representation is no longer acceptable for practical use, as the same absolute error may be minor for a flood peak and excessive for a low flow [44]. It is therefore more appropriate to calculate the errors using the observed flow/simulated flow ratio. The expression for the uncertainty associated with the flow calculated by a hydrological model is given by Eq. 5:

$$I = \frac{Q_{observed}}{Q_{simulated}} \quad (5)$$

The deviation associated with the simulated flow rate can be quantified using the Nash criterion, where I represents the uncertainty, $Q_{observed}$ represents the observed flow, and $Q_{simulated}$ represents the simulated flow. A satisfactory representation of catchment dynamics,

assuming stationarity in its behavior, is achieved when the model meets this criterion.

The efficiency of the model is determined by how closely the estimated flows align with the observed flows, indicated by a Nash criterion value close to 100%. A criterion below 60% indicates unsatisfactory agreement between the observed and simulated hydrographs. However, the Nash criterion is not limited to this threshold [55]. This dimensionless criterion allows for the assessment of the quality of the fit and facilitates comparisons across basins with varying magnitudes of flow. When analyzing simulation results, the focus is on the performance of the models during both calibration and validation. Calibration performance alone may not fully reflect the models' true simulation capabilities, which are better assessed through validation [56]. In the basin, calibration was performed for the period 1981–1990 (the year 1980 (over the 365 days) used as a warm-up period), followed by validation for the periods 1991–2000 and 2001–2010.

Model calibration/validation method

Calibration is the process of optimizing the parameters of a model to obtain the best fit to observed data, specifically the observed flow data. On the other hand, model validation is the process of assessing the adequacy of the calibrated model by testing its performance on data that were not used for calibration, typically extending beyond the calibration period. The GR4J (Rural Engineering with 4 parameters Daily) model, which has four parameters, can be calibrated using various techniques. The user can choose the optimization function for manual calibration or self-calibration mode [45, 47]. The selected optimization function aims to determine the most appropriate parameters through iterative processes for a given catchment. In this study, the GR4J model is calibrated using a self-calibration process with the help of the Microsoft Excel solver. This process uses an initial parameter set, often referred to as the "seed", and refines the range of metaparameters [52]. The model is then run, and the objective function is calculated for each set of metaparameter values. For the calibration and validation of the GR4J model in this study, flow data from the period 1981 to 2000 were utilized, with two sub-periods considered. The choice is justified not only by the availability of climatological data and measured flow data for comparison with calculated flow rates, but also by the opposition between the 1981–1990 sub-period (inserted in the dry period) and the 1991 period. – 2010 (almost wet period) marked by the return of more or less excess rainfall. The flow time series at the Simenti station were divided into three periods: the warm-up period, the calibration period, and the validation period. It is recommended to have a warm-up period of at least 3 months to 1 year

before the start of the calibration and validation years. In this case, a one-year warm-up period from January 1, 1981, to December 31, 1981, was chosen to ensure a proper representation of soil moisture and groundwater reserves in the basin. The selected sub-periods were homogeneous and corresponded to either a dry sequence or a wet sequence, determined through analysis of the stationary breaks in the rainfall and flow time series. The first ten years (1981–1990) were used for calibration, the subsequent ten years (1991–2000) for validation 1, and the final ten years (2001–2010) for validation 2. Taking into account the availability of data and the equality of the validation length compared to the calibration length, it was preferred to split the validation period which goes from 1991 to 2010 into two sub-periods of 10 years each and on which model validation was carried out.

The assessment of observed and simulated flows over wet and dry sub-periods using the GR4J model and the Nash–Sutcliffe criteria is crucial for understanding the model’s performance and reliability. Figure 3 shows the variability of experiential and simulated flows, allowing for a detailed comparison during different sub-periods, such as calibration and validation. By analyzing the wet and dry sub-periods separately, researchers can gain insights into the model’s ability to capture the hydrological response under different hydroclimatic conditions. This analysis helps identify any biases or limitations in the model’s representation of flow dynamics during wet or dry periods. It provides valuable information for water resource management, as the performance of the model can differ under varying climatic conditions. The use of various Nash–Sutcliffe criteria enhances the evaluation of model performance. These criteria, which measure the contract among experiential and simulated flows,

provide a quantitative calculation of the model’s accuracy. By applying dissimilar Nash–Sutcliffe criteria, such as the daily, monthly, or annual criteria, researchers can assess the model’s performance at different temporal scales. This analysis helps identify potential discrepancies between observed and simulated flows and guides the refinement of the model calibration. The comparison of observed and simulated flows over wet and dry sub-periods provides valuable insights into the GR4J model’s performance under different hydrological conditions. It allows for a comprehensive evaluation of the model’s ability to capture flow variability and provides a basis for further model improvement. This information is vital for effective water management and decision-making, as it helps understand the model’s reliability in simulating flows during wet and dry periods.

Acquisition of future precipitation and temperature data and simulation

The Latest simulations from the Coupled Model Inter-comparison Project Phase 6 (CMIP6), as presented in the IPCC’s 6th Assessment Report, were utilized for the climate projections in this study. A total of 18 climate models from CMIP6 were employed. To account for the natural variability and systematic biases inherent in individual models, the ensemble mean of these models was calculated for the analyses [57]. The data were further corrected using the modified quantile method [58], which helps improve the quality and resolution of regional climate change estimates worldwide. The CMIP6 models provide historical data and potential future scenarios of radiative forcing based on greenhouse gas emissions [59]. These scenarios, known as Shared Socioeconomic Pathways (SSPs), include detailed reports of upcoming people,

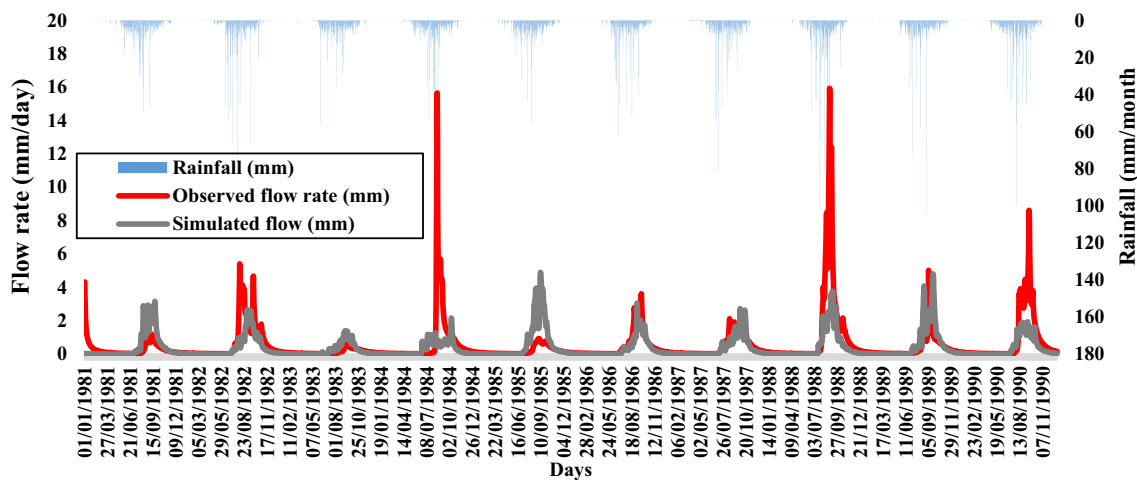


Fig. 3 Daily hydrograph of observed and simulated flows for the calibration period (1981–1990) at the Simenti gauging station

budget, technical expansion, and other social factors. They offer five dissimilar pathways that represent how the world can address the challenges of climate change in defined of variation and justification [60]. SSPs provide a framework for examining the potential challenges associated with weather variation adaptation and moderation [61]. The current research, rainfall datasets from the particular model were extracted in netCDF format for the study area. Arc GIS 10.5 was used to find precise location information. However, focus of this study was primarily on two scenarios: SSP245 (medium adaptation challenge, medium mitigation challenge) and SSP585 (low adaptation challenge, high mitigation challenge) [62]. Historical data covering the period 1985–2014 and future data spanning 2021–2100 were chosen for analysis.

The data are first evaluated on the territory of Senegal, the South-East zone in particular, and were

corrected using the modified quantile method according to Bai et al. [58] which give good results compared to other methods. For temperatures, the quantile method applied is the one that uses the difference. For rainfall, the quantile method applied is that which uses a Delta Multiplicative Factor. The model data are used and corrected individually by quantile methods before the ensemble averages are used. In the Gambia basin, compared to the observed data from the Kedougou station, the correlation coefficient of the outputs of the multi-model ensemble whose biases are corrected is greater than 0.96% for temperatures and 0.62% for precipitation, while it was around 0.9% for temperatures and 0.31% for precipitation between the observed data and the uncorrected data. Beyond bias correction, the unique use of the average ensemble will make it possible to circumvent the divergence of climate models for

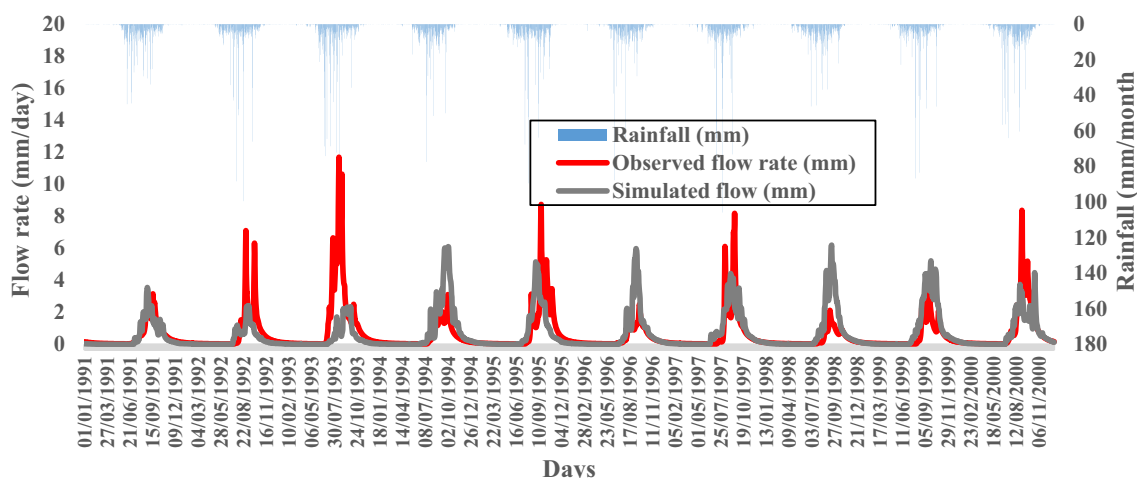


Fig. 4 Daily hydrograph of observed and simulated flows for validation period 1 (1991–2000) at the Simenti gauging station

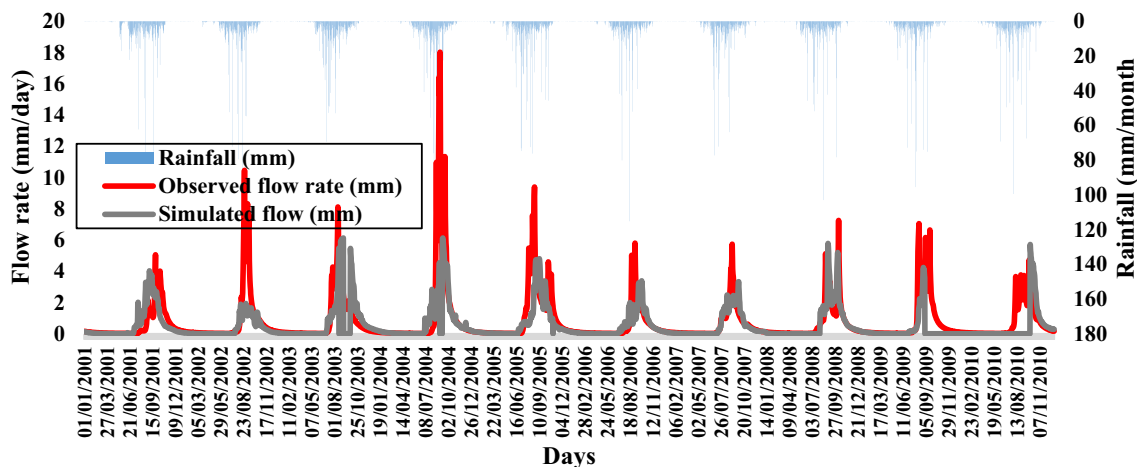


Fig. 5 Daily hydrograph of observed and simulated flows for validation period 2 (2001–2010) at the Simenti gauging station

the future horizon and the single future trajectory (the average ensemble) will mask the uncertainties on the future climate. For future projections, the multi-model ensemble used in this study is therefore more reasonable than a single model [63].

Results and discussion

Variability of observed and simulated flows over wet and dry sub-periods in calibration and validation with the GR4J model using the various Nash–Sutcliffe criteria

Figures 3, 4, and 5 provide important insights into the analysis of this basin using GR4J model. Figure 3 depicts the variability of precipitation, which is a crucial input for hydrological modeling. Understanding the temporal and spatial patterns of rainfall is vital for accurately simulating flow in the catchment. Figure 3 allows researchers and water managers to assess the distribution, incidence, and strength of precipitation events, which can have an important effect on the hydrological response in the basin. Figure 4 showcases a comparison between observed and simulated flows. This evaluation is essential for assessing the performance of the GR4J model in replicating the hydrological behavior of the Gambia basin. By visually comparing the observed and simulated flows, researchers can identify any discrepancies or biases in

the model outputs. This analysis helps to understand how well the model captures the temporal variations and magnitudes of the actual flows in the basin. The figure provides a comprehensive assessment of the model's capability to reproduce the observed hydrological processes and informs decisions related to water management and planning. Figure 5 presents the probabilities of non-exceedance derived from the GR4J model using the calculated Nash–Sutcliffe criteria. This figure offers valuable information about the reliability and confidence of the model's predictions. It provides a probability distribution of flow values, indicating the likelihood of different flow levels occurring in the future. These probabilities are useful for decision-making processes, as they assist in understanding the range of possible flow scenarios under different conditions. Water managers can utilize this information to evaluate potential risks and develop appropriate strategies for sustainable water resource management. In summary, Figs. 3, 4, 5 and 6 play a crucial role in the assessment and analysis of the Gambia basin using the GR4J model. They provide insights into precipitation variability, model performance in simulating flows, and the probabilities of non-exceedance. These visual representations enhance our understanding of the hydrological processes in the basin, guide decision-making, and contribute to effective water resource

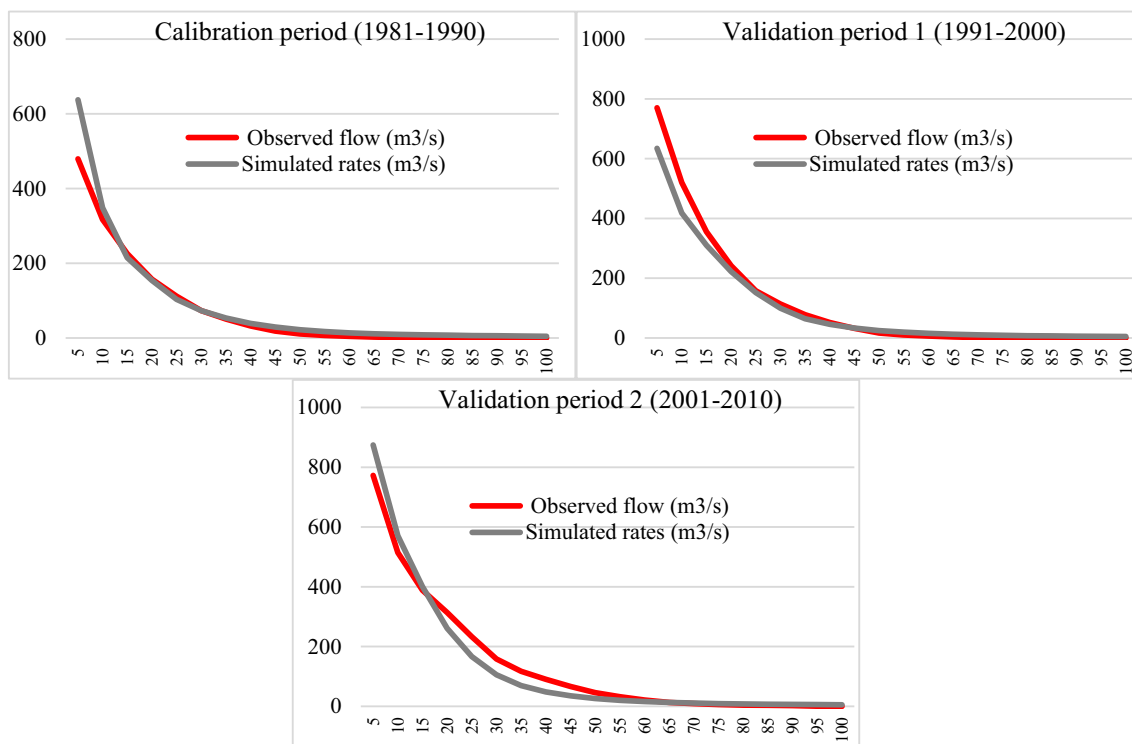


Fig. 6 Flow duration curves comparing observed and simulated outputs at the Simenti gauging station

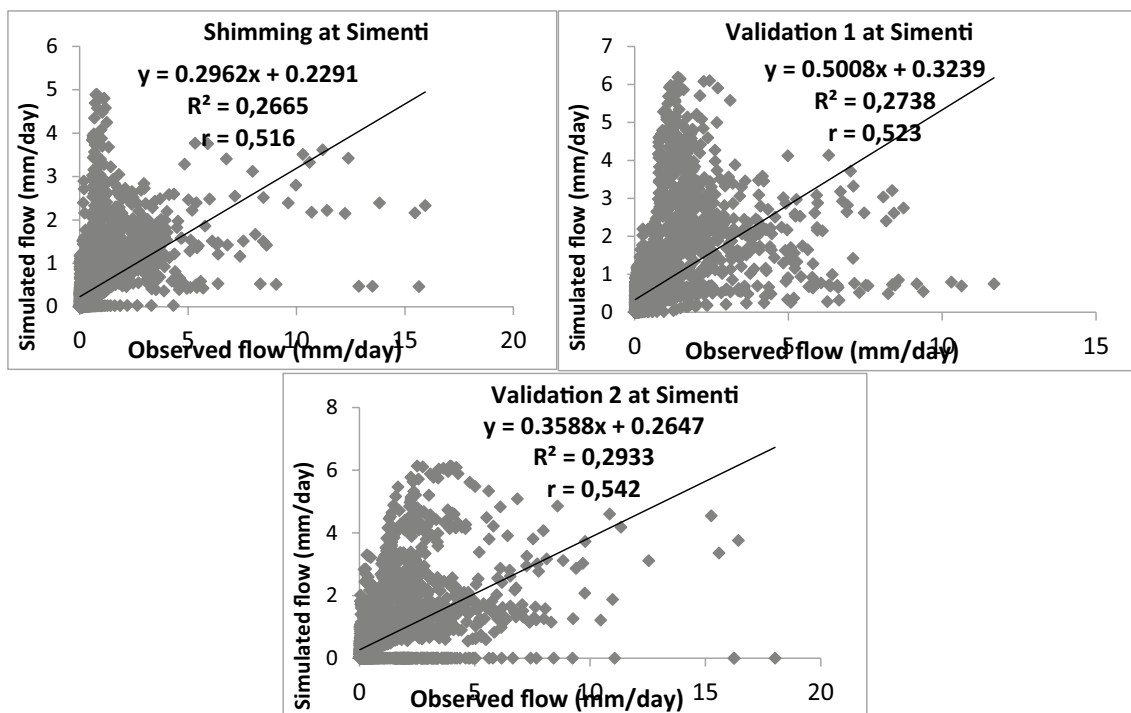


Fig. 7 Scatterplots of measured runoff versus simulated runoff for the calibration (1981–1990) and validation (1991–2000 and 2001–2010) periods at the Simenti gauging station

management. These flow duration curves comparing the observed and simulated flow at the Simenti station show a better relationship in calibration and validation (Fig. 6) than Daily hydrograph (Fig. 5). These flow duration curve results also indicate that in the basin, the calibration set performs best for flow, followed by validation set 1, while validation set 2 has the worst performance in simulation.

According to Fig. 7, the GR4J model exhibited better performance during the validation phases compared to the calibration period. The correlation coefficient (*r*) values for the validation periods of 1991–2000 and 2001–2010 were 0.523 and 0.542, respectively, while the coefficient for the calibration period was 0.516. It is worth exploring whether enhancing the GR4J model’s ability to match a proportional fraction of soil moisture could further improve its performance. However, this assumption requires further investigation in future research. In the GR4J model, the soil moisture fraction is calculated as the difference between available soil moisture and field capacity. In nature, soil moisture reaches saturation levels within 2 to 4 days, after which it gradually approaches field capacity through the process of soil water drainage. The GR4J model does not explicitly require an upper limit for saturation soil moisture, which may contribute to its effectiveness in simulating flow.

In statistics, a Q–Q (quantile–quantile) plot, which is a graphical method for comparing two probability distributions by displaying their quantiles versus quantiles, is used (Fig. 8). This normal Q–Q plot curves indicated that our sample is biased, with the points not aligning along the line.

Table 1 shows the outcomes of the model performance criteria during the calibration and validation phases. The criteria used include Nash–Sutcliffe efficiency (Nash), bias in whole flow volume (*Q*), and efficiency for each objective function applied to the gauging station to assess model performance. The research investigation of this study is presented in Table 1. The scatterplots of observed and simulated daily hydrographs are shown in Figs. 1, 2, and 3, it is marked that the Nash–Sutcliffe criteria, including Nash–Sutcliffe (*Q*), Nash–Sutcliffe (*VQ*), and Nash–Sutcliffe (*ln(Q)*), yielded acceptable results. An acceptable relationship was observed among the observed and simulated flow data, with the Nash–Sutcliffe (*Q*) criterion placing significant importance on the differences between simulated and observed flood flows. The values obtained were 0.623, 0.711, and 0.578 during the calibration period (1981–1990) and the validation periods (1991–2000 and 2001–2010), respectively. The Nash–Sutcliffe (*ln(Q)*) criterion, which effectively

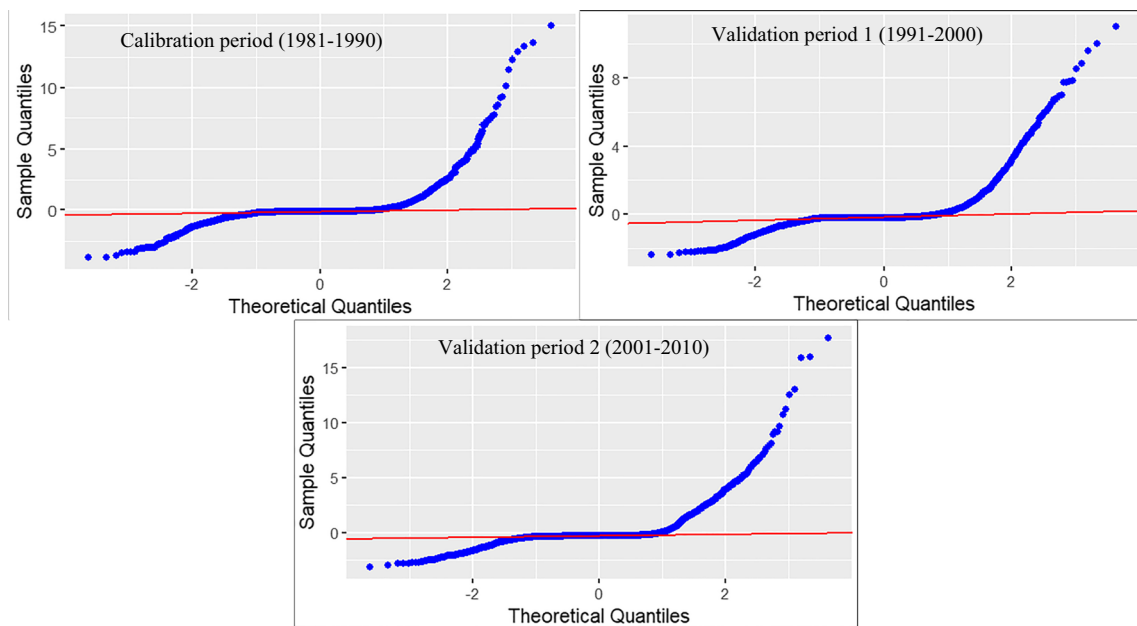


Fig. 8 Quantile–quantile plot of residuals of measured runoff versus simulated runoff for the calibration (1981–1990) and validation (1991–2000 and 2001–2010) periods at the Simenti gauging station

Table 1 Model performance criteria in the calibration and validation phase

Calibration period (1981–1990)	Efficiency criteria
Nash–Sutcliffe (Q)	0.623
Nash–Sutcliffe (VQ)	0.778
Nash–Sutcliffe (ln(Q))	0.694
Balance sheet	1.314
Validation period 1 (1991–2000)	Efficiency criteria
Nash–Sutcliffe (Q)	0.711
Nash–Sutcliffe (VQ)	0.827
Nash–Sutcliffe (ln(Q))	0.711
Balance sheet	0.997
Validation period 2 (2001–2010)	Efficiency criteria
Nash–Sutcliffe (Q)	0.578
Nash–Sutcliffe (VQ)	0.800
Nash–Sutcliffe (ln(Q))	0.737
Balance sheet	0.926

represents changes in the hydrological system during low-flow periods and provides better performance for low flows, yielded values of 0.694, 0.711, and 0.737 in the calibration period and the validation periods, respectively. To assign similar weight to the simulation of flood and low-water flows (or the simulation of average flows),

the Nash–Sutcliffe (VQ) criterion was utilized, resulting in values of 0.778, 0.827, and 0.800 during the calibration period and the validation periods, respectively, during the calibration period (1981–1990) and the validation periods (1991–2000 and 2001–2010).

Table 2 Average flows observed and simulated (mm) by the GR4J model in the Casamance basin at Simenti

Period	Calibration (1981–1990)			Validation 1 (1991–2000)			Validation 2 (2001–2010)		
	Flow observed	Simulated flow	Difference	Observed flow rate	Simulated flow	Difference	Observed flow rate	Simulated flow	Difference
Average flow	0.527	0.385	0.142	0.603	0.626	– 0.023	0.756	0.536	0.220
High water	0.856	1.064	– 0.208	1.338	1.216	0.122	1.558	1.088	0.470
Low water	0.046	0.139	– 0.094	0.112	0.161	– 0.049	0.178	0.137	0.041

Calculation of the errors using the observed flow/simulated flow ratio gives an uncertainty of around 1.314 for the calibration period (1981–1990), indicating a slight underestimation of flows by the model compared with observed flows. As for the validation periods, these errors are 0.997 and 0.926, respectively, in 1991–2000 and 2001–2010, indicating a slight overestimation of flows by the model compared with observed flows. We note here that the values of r and efficiency are close for the three periods. Overall, flows at the Simenti gauging station are both slightly underestimated and slightly overestimated by the model for all objective functions, depending on the weights used. Compared with all the objective functions, Nash–Sutcliffe (Q) shows the poorest performance in terms of volume bias for the different calibration and validation periods.

Comparisons of correlation coefficients, volume bias, and efficiency results indicate that the GR4J model provided a better estimation of simulated flow when the Nash–Sutcliffe (VQ) objective function was used. Similar findings were observed in numerous calibration processes conducted in various catchments in Africa, where the Nash–Sutcliffe (VQ) objective function yielded improved estimates of daily flows, timing, and volume ratios (Vaze et al., 2011). It is noteworthy that the model's performance showed a shift from underestimation during calibration to overestimation during validation at the Simenti station. Interestingly, in absolute terms, the model performed better during validation than during calibration when using the Nash–Sutcliffe (VQ) objective function. Figure 3 depicts a curve indicating that, in certain years, the model failed to capture flows greater than 15 mm during both the calibration and validation periods at the Simenti station. Consequently, larger water volume deficits and even greater increases in water volume were observed during the validation period at the Simenti station. These disparities in volume could be attributed to variations in flow between the calibration and validation periods. Specifically, the mean annual flow recorded in the calibration period was 0.385 mm, while it increased to 0.603 mm in validation period 1 and further to 0.756 mm in validation period 2 (Table 2). As for the average flow simulated by the model, it is 0.142 mm in the calibration

period (i.e., 0.142 mm behind the observed flow), 0.626 mm in validation period 1 (i.e., 0.023 mm above the observed flow) and 0.536 mm in validation period 2 (i.e., 0.220 mm behind the observed flow).

Similarly, the mean high-water discharge observed in the calibration period is 0.856 mm, whereas it increases to 1.338 mm in validation period 1 and 1.558 mm in validation period 2, even if the increase is not significant. As for the model-simulated mean high-water discharge, it is 1.064 mm in the calibration period (i.e., 0.208 mm greater than the observed discharge), 1.216 mm in validation period 1 (i.e., 0.122 mm less than the observed discharge) and 1.088 mm in validation period 2 (i.e., 0.470 mm less than the observed discharge). For the low-water period, the simulated flow is greater than the observed flow in calibration (with a value of 0.094 mm) and in validation 1 (0.049 mm), while in validation 2, a delay is noted with a value of 0.041 mm.

The correlation between observed flows and simulated flows (Table 3) shows better correlation coefficients for validation than for calibration at Simenti. However, the results obtained show that the GR4J model is an efficient model for simulating daily flows, especially in the Gambia basin at the Simenti station. The simulated values are close to those observed and attest to the model's validity. The analysis of the different performances (Table 3) shows first of all that the validation performances are better than the calibration performances. These performances are 69.8% for the calibration period (1981–1990), 75% for validation period 1 (1991–2000) and 70.5% for validation period 2 (2001–2010) at the Simenti station. Uncertainties are low and are of the order of 0.142 mm over the calibration period (i.e., underestimation of

Table 3 Correlation between observed and simulated flows, average performance and uncertainties in calibration and validation in the Casamance basin at Simenti

Station	Calibration	Validation 1	Validation 2
Correlation coefficient	0.516	0.523	0.542
Average performance (%)	69.8	75.0	70.5
Average deviation in mm	0.142	– 0.023	0.220

flows by the model), -0.023 over validation period 1 (i.e., overestimation of flows by the model) and 0.220 over validation period 2 (i.e., underestimation of flows by the model). Furthermore, it is important to note the differences in rainfall–runoff ratios during the calibration and validation periods in the basin. The average rainfall for calibration period 1, calibration period 2, and validation period is 1158 mm, 1203 mm, and 1289 mm, respectively. These statistics indicate varying relationships between rainfall and runoff in the basin during these periods. Additionally, there is a notable increase in both rainfall and runoff observed during the validation period, particularly during the high-water period at the Simenti station. Considering these characteristics, it is possible that the parameters calibrated to capture the phenomena during the calibration period might not accurately reproduce the flow during the validation period. One factor that influences this is the parameter associated with groundwater exchange, which affects conveyance. During the calibration period, the precipitation exceeds the flow at the Simenti station. The presence of both negative and positive parameter values, as well as their magnitudes, can be attributed to the differences in the time periods between calibration and validation. This emphasizes the importance of having similar climatic conditions between the calibration and validation periods, as parameters derived from a wetter (or drier) period may not be applicable to a drier (or wetter) period.

Future hydrological trends

Future annual hydrological trends

The upcoming forecasts were evaluated over three 20-year periods: near future (2021–2040), medium future (2041–2060 and 2061–2080), and far future (2081–2100), using the 30 year control period of 1985–2014. The choice of this division into time horizons is explained by

the need to generally have 3 horizons (near, medium and distant), through which hydroclimate trends are studied and compared. The data from the three future horizons (each 20 years long) are compared to that of the 30 year period (1985–2014), a period which constitutes a reference in climatology. The use of 30 year periods as a reference period is based on a scientific statistical convention that a minimum of 30 data points would be required to determine an average. Thus, calculating an average of data over a period of 30 years is the preferred method for representing the average state of a climate. This helps ensure that what is described is actually an aspect of the climate system and not the more variable experience of weather conditions. Annual averages can vary greatly from year to year, whereas a 30 year average eliminates much of this variation and sheds more light on common conditions [64, 65].

To characterize the annual variability of future flow in the Gambia basin at the Simenti station, characteristic annual flow values are shown in Table 4 and Fig. 9. As observed data for the different hydrological components of the basin were available, they were used as well as the model outputs as baseline or reference data, allowing a comparison of the flow components for the future scenarios with the simulated historical values. At the Simenti station, where the interannual modulus over the reference period (1985–2014) is 168 m³/s for observed flows and 187 m³/s for simulated flows, the future period (2021–2100) recorded a modulus of 98.3 m³/s under the SSP245 scenario, i.e., an average deviation of -41.5% compared with the observed flow over the reference period, and a modulus of 91.4 m³/s under the SSP585 scenario, i.e., an average deviation of - 45.5% compared with the observed flow over the reference period.

The variations in rainfall and temperature that controlled to variations in possible flow are presented in

Table 4 Future changes in flow (in %) on an annual scale over the four (04) future periods at the Simenti station

SSP245	1985–2014	2021–2040	Change in %	2041–2060	Change in %	2061–2080	Change in %	2081–2100	Change in %
Flow rates	168	108	- 35.8	94.0	- 44.0	98.3	- 41.4	93.2	- 44.4
Precipitation	1281	1134	- 147	1107	- 174	1109	- 172	1113	- 168
Average temperature	28.0	29.0	0.99	29.6	1.65	30.3	2.27	30.7	2.71
PET	14.7	1511	44.4	1540	73.8	1569	102	1588	121
SSP585	1985–2014	2021–2040	Change in %	2041–2060	Change in %	2061–2080	Change in %	2081–2100	Change in %
Flow rates	168	119	- 29.1	108	- 35.7	74	- 55.6	64	- 61.6
Precipitation	1281	1141	- 140	1128	- 153	1058	- 223	1031	- 250
Average temperature	28.0	29.1	1.08	30.2	2.26	31.6	3.66	33.2	5.22
FTE	1467	1515	48.8	1568	101	1631	164	1700	234

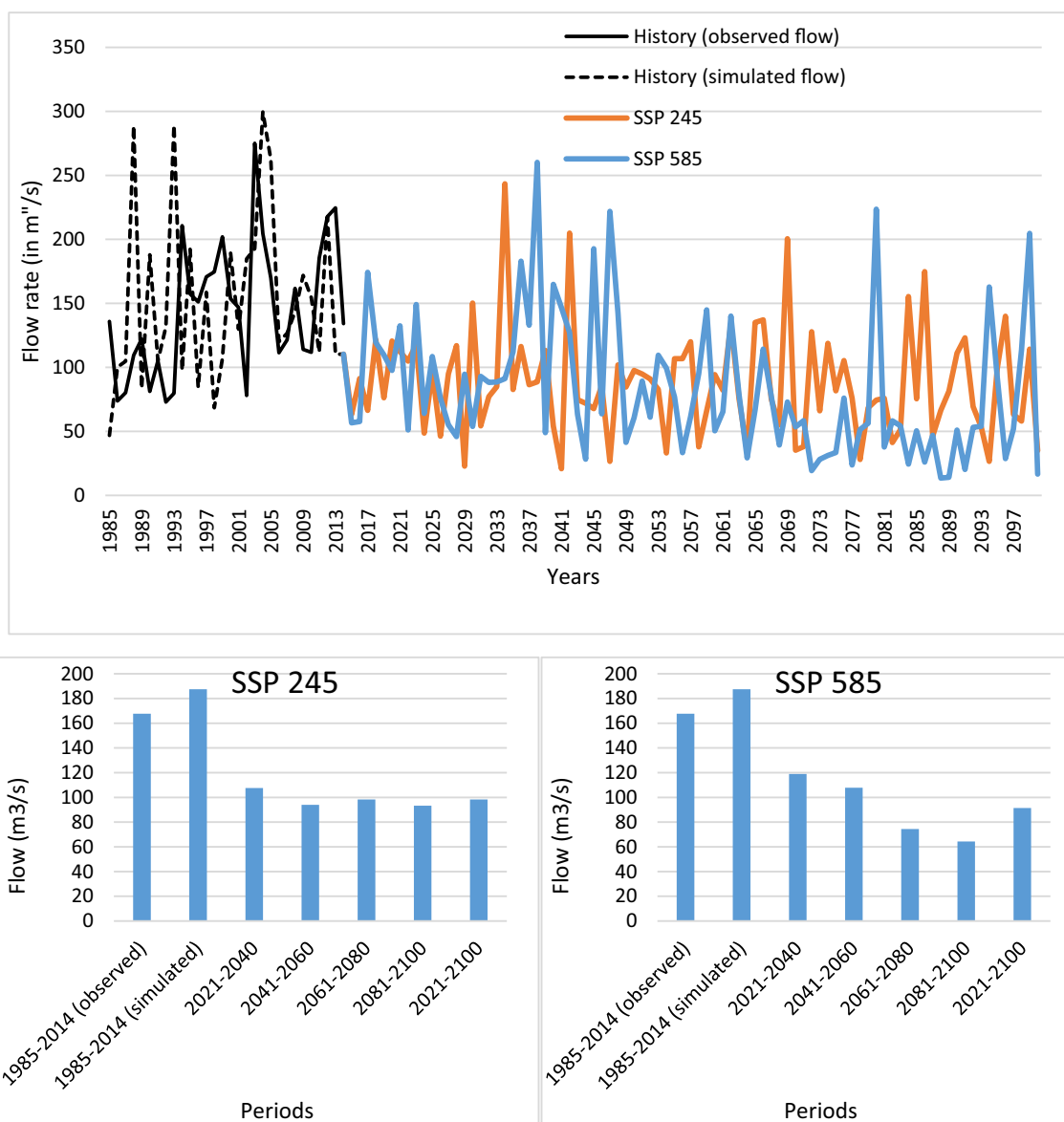


Fig. 9 Historical and projected annual flow trends from 1985 to 2100 according to the SSP245 and SSP585 scenarios at the Simenti station

Table 4. The analysis of runoff over the future period shows a decrease in runoff over the different sub-periods under both scenarios, in phase with the decrease in rainfall. There is a constant downward trend in the predictable hydrological variations for entirely scenarios. The decrease in discharge over the upcoming period diverse considerably between the four scenarios. Ranked from smallest to largest over the horizons, this decrease in flow, compared with the flow observed over the reference period, is of the order of -35.8%, - 44.0%, - 41.4% and - 44.4%, respectively, for the horizons 2040, 2060, 2080 and 2100 under the SSP245 scenario. For the SSP585 scenario, this reduction over these four

horizons is, respectively, - 29.1%, - 35.7%, - 55.6% and - 61.6%. While for the first two horizons (2040 and 2060), the decline is greater under the SSP245 scenario, for the last two horizons (2080 and 2100), the decline is greater under the SSP585 scenario.

To better understand future flow conditions in the basin, check time series trends and identify possible break periods over the future period (2015–2100), the Mann–Kendall and Pettitt tests are applied to the data, respectively. The results are presented in Table 5 and reveal large fluctuations and statistically significant trends. Unlike the historical period (1985–2014), runoff showed decreasing trends in the future period (2015–2100). This

Table 5 Average monthly flow values for the reference and future periods at the Simenti station

	SSP245			SSP585		
	1985–2014	2021–2100	Difference (%)	1985–2014	2021–2100	Difference (%)
January	20.7	25.4	22.6	20.7	24.4	17.6
February	8.94	16.1	80.3	8.94	15.5	73.9
March	3.00	11.4	278	3.00	11.0	267
April	1.63	8.48	421	1.63	8.27	408
May	0.66	6.66	911	0.66	6.52	889
June	3.81	5.51	44.5	3.81	5.41	42.1
July	73.1	8.56	− 88.3	73.1	8.63	− 88.2
August	352	104	− 70.3	352	87.1	− 75.2
September	683	401	− 41.3	683	360	− 47.3
October	420	298	− 29.0	420	295	− 29.9
November	120	116	− 3.52	120	111	− 7.62
December	48.8	47.9	− 1.77	48.8	45.5	− 6.68
Rainy season	306	163	− 46.6	306	151	− 50.7
Dry season	29.1	33.1	13.7	29.1	31.7	9.00
Year	168	98.3	− 41.4	167.7	91.4	− 45.5

Table 6 Mann–Kendall test and Pettitt test on hydroclimatic parameters over the past period (1986(2014) and future period (2015–2100) at the Simenti station

	Mann–Kendall test				Pettitt test				
	Kendall Tau	p-value (bilateral)	Alpha	Sen slope	Breakup date	p-value	Average before break	Average after breakage	Rate of change
1985–2014 (observed)	0.310	0.016	0.05	2.608	1993	0.003	95.6	166	73,1
1985–2014 (simulated)	0.166	0.205	0.05	1.101	1999	0.152	136	168	23,4
SSP 245	− 0.087	0.236	0.05	− 0.212	2057	0.653	89.5	83,9	− 6,2
SSP 585	− 0.292	< 0.0001	0.05	− 0.698	2059	< 0.0001	100.7	62,5	− 37,9

downward trend is more significant under SSP585 than SSP245, with a Kendall Tau of $-0.087 \text{ m}^3/\text{s}/\text{year}$ and $- 0.292 \text{ m}^3/\text{s}/\text{year}$ under SSP 245 and SSP 585, respectively. Pettitt, it indicates a break noted in 2057 on the SSP245 and 2059 on the SSP585, with a respective drop of 6.2% on the SSP245 and 37.9% on the SSP585.

Future monthly hydrological trends

The flow characteristics on a monthly scale in basin area at the Simenti station over the situation period and the upcoming period are shown in Table 6 and Figs. 8, 9. The river regime at this station is therefore characterized by a 3 month high-water period and a 9 month low-water period. The regime of the Gambia catchment at Simenti is characterized by a maximum in September ($683 \text{ m}^3/\text{s}$ over the reference period, $401 \text{ m}^3/\text{s}$ under the SSP245 scenario and $360 \text{ m}^3/\text{s}$ under the SSP585 scenario) and

a minimum in May ($0.66 \text{ m}^3/\text{s}$ over the reference period, $6.66 \text{ m}^3/\text{s}$ under the SSP245 scenario and $6.52 \text{ m}^3/\text{s}$ under the SSP585 scenario): this is a unimodal regime. The high-water period lasts 3 months, making it a pure tropical regime.

The average monthly rates of change in flow below the two dissimilar SSP scenarios for the dissimilar times are presented in Figs. 8, 9. Overall, there is a descending trend in flow for the months July to December ahead, but the decrease varies considerably from month to month. In general, the greatest decrease is noted over the far upcoming under both scenarios and occurs during the high-water period. On a monthly scale, the decrease in flow is expected to be greatest in August and September in both the near and distant future. Moreover, the maximum value of river discharge has changed from September in the historical period and the near future

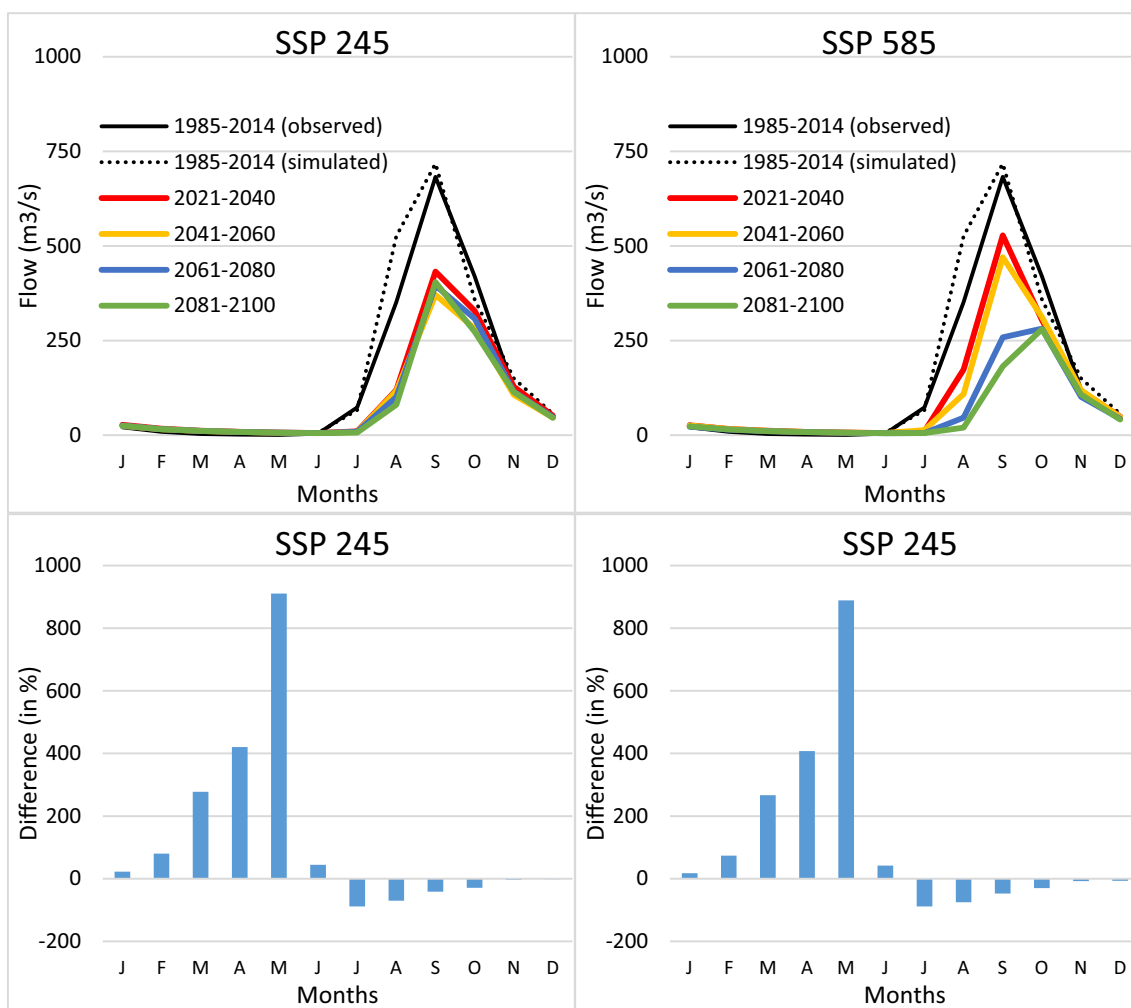


Fig. 10 Comparative evolution of the flow regime over the four future periods compared with the reference period at the Simenti station

(2021–2040) and medium future 1 (2041–2060) to October in the medium future 2 (2061–2080) and far future (2081–2100) under the SSP585 scenario (Fig. 8).

The range of deviations for the change in projected future flow is shown in Fig. 10. A disparate evolution is associated with the change in flow, with a large difference between high-water months with negative deviations (decrease in future flow) and low-water months with positive deviations (increase in future flow). The rainy seasons (high-water period) will record a fall of around – 46.6% under SSP245 and – 50.7% under SSP585. Conversely, dry seasons (low-water periods) will increase by 13.7% under SSP245 and 9.0% under SSP585.

An analysis of annual flow changes in the Gambia basin during the historical period reveals an uneven distribution of monthly flow at the Simenti station due to the seasonal influence of low flow originating from the water table. This uneven distribution has implications for the

hydrological and ecological processes within the basin. The anticipated decrease in flow, coupled with the high uncertainty of future floods, will significantly impact the hydrological resource system and weaken its overall functioning. Understanding the changes in the contribution of different hydrological components to climate change within the river basin is of great importance. This study aimed to simulate changes in the main hydrological components relative to a baseline period (1985–2014) using a model to represent future scenario periods. By analyzing and comparing the simulated flow components, insights can be gained into the potential changes in the hydrological system under different climate change scenarios. Figure 11 shows that in the near, medium and distant future, discharge decreases under SSP245 and SSP585, respectively, compared with the control period (1985–2014). The changes and the magnitude of the changes in discharge are very different are consistent in the different

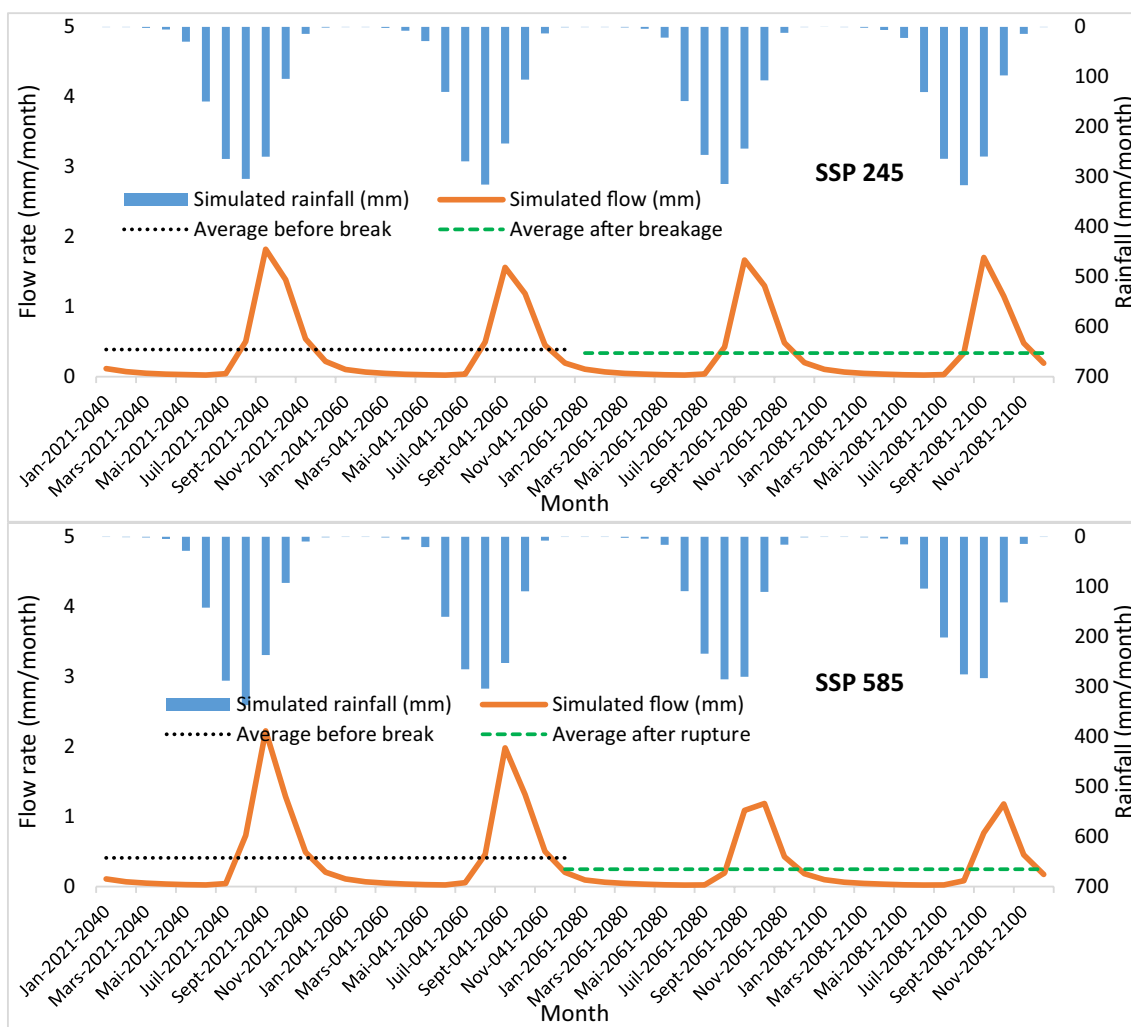


Fig. 11 Monthly trends in runoff and rainfall over the four future periods at the Simenti station

scenarios with rainfall. The Gambia basin, located in the West African region, exhibits hydroclimatic variability that aligns with the projections of the Intergovernmental Panel on Climate Change (IPCC). Projections from climate models indicate a decrease in average monthly flows at the Simenti station under two scenarios (SSP245 and SSP585) for future time horizons. These findings suggest that surface water resources in the catchment areas of the basin are expected to continue declining throughout the twenty-first century, particularly under the more severe SSP585 scenario. The vulnerability of the Gambia basin to climate change is evident, given the projected greater reduction in rainfall. The observed trends in water resources align with similar findings in other regions, highlighting the extreme scenarios presented by CMIP6. Runoff in the Gambia basin is primarily influenced by rainfall, and its seasonal changes correspond to those of precipitation patterns projected by climate models. The

results obtained were based on the use of the GR4J global hydrological model, which is relatively simple and relies on four parameters. Utilizing a distributed hydrological model could potentially enhance the accuracy and reliability of these results. Furthermore, using the average ensemble alone will certainly make it possible to circumvent the divergence of the climate model for the future horizon, but this will mask the uncertainties about the future climate. In order to encompass the uncertainties of future climate, utilizing a substantial climate ensemble is imperative. Nonetheless, merely calculating its mean does not guarantee effectively informing water managers.

Discussion

The observed and simulated hydrographs exhibit similar patterns, indicating a good match between the two datasets during the calibration and validation periods. However, there are instances where the simulated peak flows

are either underestimated or overestimated over a few years. The correlation between observed and simulated flows shows better coefficients for validation compared to calibration at the Simenti station. Nevertheless, the results demonstrate that the GR4J model is effective in simulating daily flows, particularly in the Gambia basin at the Simenti station. The simulated values closely align with the observed values, confirming the validity of the model. Analysis of uncertainties reveals relatively low values, approximately 0.142 mm during the calibration period (indicating flow underestimation by the model), -0.023 during validation period 1 (indicating flow overestimation by the model), and 0.220 during validation period 2 (indicating flow underestimation by the model). These uncertainties, as indicated by the use of the GR4J model in the Gambia basin, align with the findings of Bodian et al. [66] in the Bafing basin and Mbaye et al. [67] in the Falémé basin. The limited length of the observed data time series, which did not capture all specific hydro-meteorological events during the calibration and validation periods, may contribute to some discrepancies between simulations and observations [68]. Additionally, the discrepancies in calculated and observed runoff can be attributed to the model's inability to account for variations in crucial factors such as soil type, vegetation, topography, human activities, and other key contributors to the runoff process [22, 67, 69]. The underestimation of peak flow may also stem from the challenge of accurately reproducing flood peaks due to their sudden onset [52]. The analysis of runoff over the future period shows a decrease in runoff over the different sub-periods under both scenarios, in phase with the decrease in rainfall and the increase in temperatures and therefore in evapotranspiration [70–73]. There is a constant downward trend in the projected hydrological changes for all scenarios. The decrease in discharge over the future period varied considerably between the two scenarios and the four periods. Ranked from smallest to largest over the horizons, this decrease in flow, relative to the flow observed over the reference period, is of the order of -35.8% , -44.0% , -41.4% and -44.4% , respectively, for the horizons 2040, 2060, 2080 and 2100 under the SSP245 scenario. For the SSP585 scenario, this reduction over these four horizons is, respectively, -29.1% , -35.7% , -55.6% and -61.6% . While for the first two horizons (2040 and 2060), the decline is greater under the SSP245 scenario, for the last two horizons (2080 and 2100), the decline is greater under the SSP585 scenario. The findings of this study are consistent with those of previous research by Mbaye et al. [67], who also observed a decrease in river flow in the Gambia basin. Similarly, Bodian et al. [74] highlighted the

decline in river flow for both the Gambia and upper Senegal basins. Global warming has been found to enhance the atmosphere's water retention capacity, leading to increased surface water and soil water loss through evapotranspiration [75]. This, in turn, has an impact on basin discharge [76, 77]. Temperature and potential evapotranspiration are among the key factors driving changes in the hydroclimate of the basin. Other factors such as atmospheric humidity, surface soil moisture, length of the growing season, net radiation, and wind characteristics also contribute significantly to changes in evapotranspiration, which subsequently affects runoff and leads to a decrease in water resources [78, 79]. In general, under climate change, it is expected that temperature and potential evapotranspiration will increase, while precipitation will decrease in the catchment. Consequently, future periods from 2021 to 2100 are projected to experience reduced discharge compared to the reference period from 1985 to 2014. These findings demonstrate the direct relationship between temperature and potential evapotranspiration and their inverse relationship with rainfall and discharge in the Gambia catchment. It is important to note that this study assumed constant land use/land cover scenarios and meteorological variables such as solar radiation, wind speed, and humidity for future periods. However, these parameters directly contribute to hydrological systems, and it may be necessary to vary them in future studies. Additionally, incorporating multiple models with different scenarios for analyzing hydrological responses to climate change can help reduce uncertainties in climate change assessments.

Climate modeling induces many uncertainties in climate analysis. It is necessary to be aware of this and take it into account to best understand the data from model outputs, as well as for the interpretation of indicators of possible changes in the future climate [80]. The first uncertainties relate to the models used. In fact, they are based on past data measured in situ. However, the quality of this measured data varies. The data regionalization method also induces statistical approximations and uncertainty persists in the modeled data despite the corrections made. There are also uncertainties linked to climate change scenarios [81, 82].

Finally, uncertainties linked to the lack of knowledge about certain processes exist. Indeed, the carbon cycle process is still poorly understood, particularly in relation to aerosols.

Furthermore, using the average ensemble alone will certainly make it possible to circumvent the divergence of the climate model for the future horizon, but this will mask the uncertainties about the future climate.

Conclusion

The GR4j model is a global model which has produced good results, the pace of the simulated hydrograph follows perfectly that observed. To summarize the advantages of the GR4j model: it does not take into account the physical characteristics of the basin; there is a low number of parameters therefore ease of calibration; it makes it possible to perfectly reproduce the observed flow; there are a limited number of simulation periods in two years. The advantages therefore lie in a better robustness during the passage from the calibration phases to the control. The application of the GR4j rainfall–runoff model in the Gambia basin has demonstrated its successful performance. This study found that despite its simple structure and limited number of parameters, the GR4j model can accurately simulate flow. However, it should be noted that increased biases in flow volume, particularly during the validation periods, indicate some errors in the input data, including rainfall and runoff. The four parameters obtained through the self-calibration process varied depending on the objective function and its weighting. However, all parameters fell within the standard range. It was observed that an independent calibration process yielded better results in terms of correlation, Nash criteria, and efficiency compared to a joint calibration process. Among the four objective functions, the Nash criteria produced the most favorable outcomes. Notably, certain parameters such as groundwater exchange and production storage exhibited variations depending on the chosen objective function. However, determining the optimal parameter set proved challenging when calibrating the model in self-calibration mode. Therefore, it is essential to analyze the sensitivity of these parameters to minimize uncertainty. It may be beneficial to explore a hybrid combination of different calibration and optimization methods to enhance the model's performance and generate improved results.

Acknowledgements

Not applicable for that section.

Author contributions

SMKS: writing original draft writing, conceptualization, formal analysis, methodology, data curation, processing of data, development of models, writing—review and editing, investigation. CF: supervision, writing original draft writing, validation, investigation, methodology, writing—review and editing. CBP: formal analysis, validation, writing original draft writing, formal analysis and writing—review and editing.

Funding

This research received no external funding.

Availability of data and materials

The datasets used and analyzed during this study are available from the corresponding author on reasonable request.

Declarations

Ethics approval and consent to participate

Not applicable for that section.

Consent for publication

Not applicable for that section.

Competing interests

The authors declare no competing interests.

Author details

¹Department of Geography, U.F.R. Sciences et Technologies, Laboratory of Geomatics and Environment, Assane Seck University of Ziguinchor, BP 523, Ziguinchor, Dakar, Senegal. ²New Era and Development in Civil Engineering Research Group, Scientific Research Center, Al-Ayen University, Thi-Qar, Nasiriyah 64001, Iraq. ³Indian Institute of Tropical Meteorology, Pune, India.

Received: 5 July 2023 Accepted: 19 January 2024

Published online: 18 February 2024

References

- Gleick PH (2003) Global freshwater resources: soft-path solutions for the 21st Century. *Science* 302:1524–1528
- Wu X, Guo S, Qian S, Wang Z, Lai C, Li J, Liu P (2022) Long-range precipitation forecast based on multipole and preceding fluctuations of sea surface temperature. *Int J Climatol* 42(15):8024–8039. <https://doi.org/10.1002/joc.7690>
- Xi Z, Xiaoming Z, Jiawang G, Shuxin L, Tingshan Z (2023) Karst topography paces the deposition of lower permian, organic-rich, marine–continental transitional shales in the southeastern Ordos Basin, northwestern China. *AAPG Bull.* <https://doi.org/10.1306/11152322091>
- Aparicio, J; Lafragua, J; Lopez, A; Mejia, R; Aguilar, E; Mejia, M. (2008). Water Resources Assessment: Integral Water Balance in Basins, phi-vii ed.; Number 14 in Technical Document; UNESCO Office Montevideo and Regional Bureau for Science in Latin America and the Caribbean: Montevideo, Uruguay
- He M, Dong J, Jin Z, Liu C, Xiao J, Zhang F, Deng L (2021) Pedogenic processes in loess-paleosol sediments: Clues from Li isotopes of leachate in Luochuan loess. *Geochim Cosmochim Acta* 299(151):162. <https://doi.org/10.1016/j.gca.2021.02.021>
- Hölzel H, Diekrüger B (2012) Predicting the impact of linear landscape elements on surface runoff, soil erosion, and sedimentation in the Wahnbach catchment. *Germany Hydrol Process* 26:1642–1654
- Yin L, Wang L, Li T, Lu S, Yin Z, Liu X, Zheng W (2023) U-Net-STN: a novel end-to-end lake boundary prediction model. *Land* 12(8):1602. <https://doi.org/10.3390/land12081602>
- Yin L, Wang L, Li J, Lu S, Tian J, Yin Z, Zheng W (1813) 2023 YOLOV4_CSPBi: enhanced land target detection model. *Land* 12:9. <https://doi.org/10.3390/land12091813>
- Yin L, Wang L, Li T, Lu S, Tian J, Yin Z, Zheng W (1859) 2023 U-Net-LSTM: time series-enhanced lake boundary prediction model. *Land* 12:10. <https://doi.org/10.3390/land12101859>
- Gong S, Bai X, Luo G, Li C, Wu L, Chen F, Zhang S (2023) Climate change has enhanced the positive contribution of rock weathering to the major ions in riverine transport. *Global Planet Change* 228:104203. <https://doi.org/10.1016/j.gloplacha.2023.104203>
- Kay AL (2021) Simulation of river flow in Britain under climate change: baseline performance and future seasonal changes. *Hydrol Process* 35:e14137
- Wang X, Wang T, Xu J, Shen Z, Yang Y, Chen A, Piao S (2022) Enhanced habitat loss of the Himalayan endemic flora driven by warming-forced upslope tree expansion. *Nature Ecol Evol* 6(7):890–899. <https://doi.org/10.1038/s41559-022-01774-3>

13. Middelkoop H, Daamen K, Gellens D, Grabs W, Kwadijk JC, Lang H, Parmet BW, Schädler B, Schulla J, Wilke K (2001) Impact of climate change on hydrological regimes and water resources management in the Rhine basin. *Clim Chang* 49:105–128
14. Qin P, Xu H, Liu M, Du L, Xiao C, Liu L, Tarroja B (2020) Climate change impacts on Three Gorges Reservoir impoundment and hydropower generation. *J Hydrol* 580:123922
15. Whitehead PG, Wilby RL, Battarbee RW, Kernan M, Wade AJ (2009) A review of the potential impacts of climate change on surface water quality. *Hydrol Sci J* 54:101–123
16. Lin X, Zhu G, Qiu D, Ye L, Liu Y, Chen L, Sun N (2023) Stable precipitation isotope records of cold wave events in Eurasia. *Atmos Res* 296:107070. <https://doi.org/10.1016/j.atmosres.2023.107070>
17. Zhang S, Bai X, Zhao C, Tan Q, Luo G, Wang J, Xi H (2021) Global CO₂ consumption by silicate rock chemical weathering: its past and future. *Earth's Future* 9(5):e1938E–e2020E. <https://doi.org/10.1029/2020EF001938>
18. Zhan P, Liu L, Yang L, Zhao J, Li Y, Qi Y, Cao L (2023) Exploring the response of ecosystem service value to land use changes under multiple scenarios coupling a mixed-cell cellular automata model and system dynamics model in Xi'an China. *Ecol Indic* 147:110009. <https://doi.org/10.1016/j.ecolind.2023.110009>
19. Wu X, Feng X, Wang Z, Chen Y, Deng Z (2023) Multi-source precipitation products assessment on drought monitoring across global major river basins. *Atmos Res* 295:106982. <https://doi.org/10.1016/j.atmosres.2023.106982>
20. Xiong L, Bai X, Zhao C, Li Y, Tan Q, Luo G, Song F (2022) High-resolution data sets for global carbonate and silicate rock weathering carbon sinks and their change trends. *Earth's Future*. <https://doi.org/10.1029/2022EF002746>
21. Clark MP, Wilby RL, Gutmann ED, Vano JA, Gangopadhyay S, Wood AW, Fowler HJ, Prudhomme C, Arnold JR, Brekke Levi D (2016) Characterizing uncertainty of the hydrologic impacts of climate change. *Current Climate Change Rep* 2(2):55–64. <https://doi.org/10.1007/s40641-016-0034-x>
22. Yonaba R, Mounirou LA, Tazen F, Koïta M, Biao AC, Zouré CO, Queloz P, Karambiri H, Yacouba H (2023) Future climate or land use? Attribution of changes in surface runoff in a typical Sahelian landscape. *Comptes Rendus Géoscience*. 35:1–28
23. Vetter T, Reinhardt J, Flörke M, Van Griensven A, Hattermann F, Huang S, Koch H, Pechlivanidis IG, Plötner S, Seidou O et al (2017) Evaluation of sources of uncertainty in projected hydrological changes under climate change in 12 large-scale river basins. *Clim Chang* 141:419–433
24. Yuan J, Wang TJ, Chen J, Huang JA (2023) Microscopic mechanism study of the creep properties of soil based on the energy scale method. *Front Mater*. <https://doi.org/10.3389/fmats.2023.1137728>
25. Eyring V, Cox PM, Flato GM, Gleckler PJ, Abramowitz G, Caldwell P, Collins WD, Gier BK, Hall AD, Hoffman FM, Hurtt GC, Jahn A, Jones CD, Klein SA, Krasting JP, Kwiatkowski L, Lorenz R, Maloney E, Meehl GA, Pendergrass AG, Pincus R, Ruane AC, Russell JL, Sanderson BM, Santer BD, Sherwood SC, Simpson IR, Stouffer RJ, Williamson MS (2019) Taking climate model evaluation to the next level. *Nat Clim Chang* 9(2):102–110. <https://doi.org/10.1038/s41558-018-0355-y>
26. Li Q, Lu L, Zhao Q, Hu S (2023) Impact of inorganic solutes release in groundwater during oil shale in situ exploitation. *Water* 15(1):172. <https://doi.org/10.3390/w15010172>
27. Knutti R, Baumberger C, Hirsch Hadorn G (2019) Uncertainty quantification using multiple models—Prospects and challenges. In: Beisbart C, Saam NJ (eds) *Computer simulation validation: Fundamental concepts, methodological frameworks, and philosophical perspectives*. Springer International Publishing, Cham, pp 835–855
28. van Vuuren DP, Edmonds J, Kainuma M, Riahi K, Thomson A, Hibbard K, Hurtt GC, Kram T, Krey V, Lamarque J-F, Masui T, Meinshausen M, Nakicenovic N, Smith SJ, Rose SK (2011) The representative concentration pathways: an overview. *Clim Change* 109(1–2):5–31. <https://doi.org/10.1007/s10584-011-0148-z>
29. Yip S, Ferro CAT, Stephenson DB, Hawkins E (2011) A simple, coherent framework for partitioning uncertainty in climate predictions. *J Clim* 24(17):4634–4644. <https://doi.org/10.1175/2011jcli4085.1>
30. Chen J, Brissette FP, Chaumont D, Braun M (2013) Performance and uncertainty evaluation of empirical downscaling methods in quantifying the climate change impacts on hydrology over two North American river basins. *J Hydrol* 479:200–214. <https://doi.org/10.1016/j.jhydrol.2012.11.062>
31. Evans JP, Ji F, Abramowitz G, Ekstrom M (2013) Optimally choosing small ensemble members to produce robust climate simulations. *Environ Res Lett* 8(4):044050. <https://doi.org/10.1088/1748-9326/8/4/044050>
32. Raju KS, Nagesh Kumar D (2014) Ranking of global climate models for India using multicriteria analysis. *Clim Res* 60(2):103–117. <https://doi.org/10.3354/cr01222Sadio>
33. Gbohoui P, Paturel J, Fowe T et al (2021) Impacts of climate and environmental changes on water resources: a multi-scale study based on Nakanbé nested watersheds in West African Sahel. *J Hydrol-Reg Stud* 35:100828. <https://doi.org/10.1016/j.ejrh.2021.100828>
34. O'Neill BC, Tebaldi C, Vuuren DPV, Eyring V, Friedlingstein P, Hurtt G, Knutti R, Kriegler E, Lamarque JF, Lowe J et al (2016) The scenario model intercomparison project (ScenarioMIP) for CMIP6. *Geosci Model Dev* 9:3461–3482
35. Pande CB et al (2024) Impact of land use/land cover changes on evapotranspiration and model accuracy using Google Earth engine and classification and regression tree modeling. *Geomatics Nat Hazards Risk* 15(1):1–29. <https://doi.org/10.1080/19475705.2023.2290350>
36. Pande CB, Moharir KN, Singh SK, Varade AM, Elbeltagi A, Khadri SFR, Choudhari P (2021) Estimation of crop and forest biomass resources in a semi-arid region using satellite data and GIS. *J Saudi Soc Agric Sci* 20(5):302–311. <https://doi.org/10.1016/j.jssas.2021.03.002>
37. Lamagat J.P., 1989. Monographie hydrologique du fleuve Gambie Collection M&M. ORSTOM-OMVG, 250 p.
38. Dione O., (1996): Evolution climatique récente et dynamique fluviale dans les hauts bassins des fleuves Sénégal et Gambie. Thèse de doctorat, Université Lyon 3 Jean Moulin, 477 p.
39. Faye C., et Mendy A. (2018): Variabilité climatique et impacts hydrologiques en Afrique de l'Ouest : Cas du bassin versant de la Gambie (Sénégal). *Environmental and Water Sciences, Public Health*.
40. AA Sow (2007). L'hydrologie du Sud-est du Sénégal et de ses Confins guinéo-maliens : les bassins de la Gambie et de la Falémé Université Cheikh Anta Diop de Dakar Thèse (PhD) p. 1232
41. Bodjrenou R (2023) Evaluation of reanalysis estimates of precipitation, radiation, and temperature over Benin (West Africa). *J Appl Meteor Climatol* 62:1005–1022. <https://doi.org/10.1175/JAMC-D-21-0222.1>
42. Nakkazi MT, Sempewo JI, Tumutungire MD, Byakatonda J (2022) Performance evaluation of CFSR, MERRA-2 and TRMM3B42 data sets in simulating river discharge of data-scarce tropical catchments: a case study of Manafwa, Uganda. *J Water Climate Change* 13(2):522–541. <https://doi.org/10.2166/wcc.2021.174>
43. Kay AL, Davies HN (2008) Calculating potential evaporation from climate model data: a source of uncertainty for hydrological climate change impacts. *J Hydrol* 358:221–239
44. Amoussou E, Totin Vodounon H, Houessou S, Trambly Y, Camberlin P, Houndenou C, Boko M, Mahe G, Paturel JE (2015) Application d'un modèle conceptuel à l'analyse de la dynamique hydrométéorologique des crues dans un bassin versant en milieu tropical humide: cas du Fleuve Mono. XXVIII Colloque de l'Association Internationale de Climatologie, Liège 17–24:2015
45. eWater Ltd (2013a, October 11). Source Scientific Reference Guide (v3.5.0) (Online: Available: <https://ewater.atlassian.net/wiki/display/SD35/Source+Scientific+Reference+Guide>)
46. Harlan D, Wangsadipura M, Munajat CM (2010) Rainfall-runoff modeling of Citarum Hulu River Basin by using GR4J. *Proc World Congress Eng* 2:1–5
47. van Esse WR, Perrin C, Booij MJ, Augustijn DCM, Fenicia F, Kavetski D, Lobligois F (2013) The influence of conceptual model structure on model performance: a comparative study for 237 catchments. *Hydrol Earth Syst Sci* 17:4227–4239. <https://doi.org/10.5194/hess-17-4227-2013>
48. Mouelhi S, Michel C, Perrin C, Andréassian V (2006) Linking stream flow to rainfall at the annual time step: the manabe bucket model revisited. *J Hydrol* 328(1–2):283–296. <https://doi.org/10.1016/j.jhydrol.2005.12.022>
49. Makhlof Z (1994) Compléments sur le modèle pluie-débit GR4J et essai d'estimation de ses paramètres. Université Paris XI Orsay, Thèse de Doctorat, p 426
50. Hamby DA (1994) A review of techniques parameters sensitivity analysis of environmental models. *Environ Monit Assess* 32:135–154

51. Dechemi N, Benkaci T, Issolah A (2003) Modélisation des débits mensuels par les modèles conceptuels et les systèmes neuro-flous » Revue des sciences de l'eau. *J Water Sci* 16(4):407–424
52. Faye C., A.A. Sow. (2014). Analyse de la variabilité des ressources en eau dans le bassin de la Falémé par modélisation hydrologique, vol. 14: 12, 9p.
53. Kouassi AM (2007) Caractérisation d'une modification éventuelle de la relation pluie-débit et ses impacts sur les ressources en eau en Afrique de l'Ouest: cas du bassin versant du N'zi (Bandama) en Côte d'Ivoire. Thèse de Docteur de l'Université de Cocody, Côte d'Ivoire, 234 p.
54. Moriasi DN et al (2015) Hydrologic and water quality models: key calibration and validation topics. *Transactions of the ASABE* 58:1609–1618. <https://doi.org/10.13031/trans.58.11075>
55. Berthier C-H (2005) Quantification des incertitudes des débits calculés par un modèle pluie-débit empirique. Mémoire de Master 2ème année Sciences de la terre spécialité Hydrologie, Hydrogéologie et sols Année 2004–2005, p 55
56. Perrin C (2000) Vers une amélioration d'un modèle global pluie-débit au travers d'une approche comparative. Thèse de doctorat, Institut National Polytechnique de Grenoble, Grenoble, France, p 518
57. Akinsanola AA, Zhou W (2019) Projections of West African summer monsoon rainfall extremes from two CORDEX models. *Clim. Dyn* 52:2017
58. Bai, Y., Liu, H., Huang, B., Wagle, M., Guo, S. (2016) Identification of environmental stressors and validation of light preference as a measure of anxiety in larval zebrafish. *BMC Neuroscience*. 17:63. Bendaoud, H. Modélisation pluie-débit par le modèle conceptuel GR2M: cas du bassin versant de l'oued zeddine, Université SAAD DAHLEB –BLIDA 1, Faculté de Technologie, Département des Sciences de l'Eau et Environnement, Mémoire, 2017, 59 p.
59. Carvalho D, Pereira SC, Rocha A (2020) Future surface temperature changes for the Iberian Peninsula according to EURO-CORDEX climate projections. *Clim Dyn* 56:123–138. <https://doi.org/10.1007/s00382-020-05472-3>
60. O'Neill BC, Kriegler E, Ebi KL, Kemp-Benedict E, Riahi K, Rothman DS, van Ruijven BJ, van Vuuren DP, Birkmann J, Kok K, Levy M, Solecki W (2015) The roads ahead: Narratives for shared socioeconomic pathways describing world futures in the 21st century. In Press, *Global Environmental Change*
61. Chen Y, Li X, Huang K, Luo M, Gao M (2020) High-resolution gridded population projections for China under the shared socioeconomic pathways. *Earth's Future* 8:e2020EF001491
62. Gidden MJ et al (2019) Global emissions pathways under different socioeconomic scenarios for use in CMIP6: a dataset of harmonized emissions trajectories through the end of the century. *Geosci Model Develop* 12(4):1443–1475. <https://doi.org/10.5194/gmd-12-1443-2019>
63. Xu C, Xu Y (2012) The projection of temperature and precipitation over China under RCP scenarios using a CMIP5 multi-model ensemble. *Atmos Ocean Sci Lett* 5(6):527–533
64. Sadio CAAS et al (2023) Hydrological response of tropical rivers basins to climate change using the GR2M model: the case of the Casamance and Kayanga-Géva rivers basins. *Environ Sci Eur* 35:113.
65. The Climate Atlas of Canada, Version 2 (July 10, 2019), using data from BCCAQv2 climate models, The Climate Atlas of Canada, Version 2 (July 10), 2019, <https://atlasclimatique.ca/guide-atlas/interpret-climate-data>
66. Bodian A, Dezetter A, Deme A (2016) Hydrological evaluation of TRMM rainfall over the Upper Senegal River Basin. *Hydrology* 3:15. <https://doi.org/10.3390/hydrology3020015>
67. Mbaye ML, Sy K, Faty B, Sall SM (2020) Impact of 1.5 and 2.0 °C global warming on the hydrology of the Faleme river basin. *J Hydrol Regl Stud* 31:100719. <https://doi.org/10.1016/j.ejrh.2020.100719>
68. Montecelos-Zamora Y, Cavazos T, Kretschmar T, Vivoni ER, Corzo G, Molina-Navarro E (2018) Hydrological modeling of climate change impacts in a Tropical River Basin: a case study of the Cauto River. *Cuba Water* 10(9):1135. <https://doi.org/10.3390/w10091135>
69. Bagré MP, Yonaba R, Sirima BA, Somé YSC (2023) Influence des changements d'utilisation des terres sur les débits du bassin versant du Massili à Gonsé (Burkina Faso)”. *Vertigo* - la revue électronique en sciences de l'environnement. <https://doi.org/10.4000/vertigo.39765>
70. Burn HB, Elnur MAH (2002) Detection of hydrologic trends and variability. *J Hydrol* 255:107–122
71. Knutti R, Furrer R, Tebaldi C, Cermak J, Meehl GA (2010) Challenges in combining projections from multiple climate models. *J Climate* 23(10):2739–2758. <https://doi.org/10.1175/2009jcli3361.1>
72. Koutsoyiannis D (2006) Nonstationarity versus scaling in hydrology. *J Hydrol* 324:239–254
73. Faye CAAS, Pande C et al (2023) Hydrological response of tropical rivers basins to climate change using the GR2M model: the case of the Casamance and Kayanga-Géva rivers basins. *Environ Sci Eur*. <https://doi.org/10.1186/s12302-023-00822-4>
74. Bodian A, Dezetter A, Diop L, Deme A, Djaman K, Diop A (2018) Future climate change impacts on streamflows of two main West Africa River Basins: Senegal and Gambia. *Hydrology* 5(1):21. <https://doi.org/10.3390/hydrology5010021>
75. Mbaye ML, Sylla MB, Tall M (2019) Impacts of 1.5 and 2.0 °C global warming on water balance components over Senegal in West Africa ? *Atmos* 10(11):712. <https://doi.org/10.3390/atmos10110712>
76. Wang H-M, Chen J, Xu C-Y, Chen H, Guo S, Xie P, Li X (2019) Does the weighting of climate simulations result in a better quantification of hydrological impacts? *Hydrol Earth Syst Sci* 23(10):4033–4050
77. Zouré CO, Kiema A, Yonaba R, Minoungou B (2017) Unravelling the impacts of climate variability on surface Runoff in the Mouhoun River Catchment (West Africa). *Land* 2023:12. <https://doi.org/10.3390/land12112017>
78. Nangombe SS, Zhou T, Zhang W, Zou L, Li D (2019) High-temperature extreme events over Africa under 1.5 and 2 °C of global warming. *J Geophys Res Atmos* 124:4413–4428. <https://doi.org/10.1029/2018JD02974>
79. Olsson J, Arheimer B, Borris M, Donnelly C, Foster K, Nikulin G, Persson M, Perttu A-M, Uvo CB, Viklander M, Yang W (2016) Hydrological climate change impact assessment at small and large scales: key messages from recent progress in Sweden. *Climate* 4(3):39. <https://doi.org/10.3390/cli4030039>
80. Pande CB (2020) Sustainable watershed development planning. In: Sustainable watershed development. SpringerBriefs in water science and technology. Springer, Cham. https://doi.org/10.1007/978-3-030-47244-3_4
81. Kandekar VU, Pande CB, Rajesh J et al (2021) Surface water dynamics analysis based on sentinel imagery and Google Earth engine platform: a case study of Jayakwadi dam. *Sustain Water Resour Manag* 7:44. <https://doi.org/10.1007/s40899-021-00527-7>
82. Pande CB, Al-Ansari N, Kushwaha NL, Srivastava A, Noor R, Kumar M, Moharir KN, Elbeltagi A (2022) Forecasting of SPI and meteorological drought based on the artificial neural network and M5P model tree. *Land* 11:2040. <https://doi.org/10.3390/land11112040>

Publisher's Note

Springer Nature remains neutral with regard to jurisdictional claims in published maps and institutional affiliations.